Wide Area Voltage Stability Assessment Based on Generator-Derived Indices Using Phasor Measurement Units

A.C. Adewole and R. Tzoneva

Abstract—The continuous increase in energy demand without a concomitant increase in generation and transmission capabilities inevitably leads to power system instability and consequently blackouts. This paper proposes and investigates the application of generator-derived Voltage Stability (VS) indices using synchrophasor measurements from dispersed Phasor Measurement Units (PMUs) for real-time monitoring and situational awareness in power systems. Three VS indices derived from the capability parameters of synchronous generators in the power system are presented, and used in the prediction of the power system's margin to voltage collapse. The proposed generator-derived VS indices were tested using the New England 39-bus benchmark test system modelled using RSCAD software. Real-time hardware-in-the-loop simulations involving a lab-scale testbed using the Real-Time Digital Simulator (RTDS), PMUs, Phasor Data Concentrators (PDCs), Programmable Logic Controller (PLC), communication network switches, and GPS satellite clock were carried out in order to test the proposed VS indices for various system operating conditions encompassing credible contingencies, increased system loading, operation of transformer Under-Load Tap-Changers (ULTCs), and generator Over Excitation Limiters (OXLs). The results obtained showed that the VS indices provided an exact snap-shot of the grid in real-time. The VS indices would be useful in the design of System Integrity Protection Schemes (SIPS) that are capable of preserving the integrity of the grid during disturbances and parametric changes, thereby preventing system blackouts.

Index Terms—**Blackout, phasor measurement units, real-time digital simulation, synchrophasors, voltage stability, wide area monitoring**

1 Introduction

The lack of new power system generating and transmission infrastructure has resulted in the operation of the existing power systems in a stressed state. This coupled with the ever growing demand for energy and interconnections, inevitably results in power system instabilities and consequently blackouts.

Post-mortem analysis of the recent blackout in North America [1] showed that it could have been prevented if the power system was monitored using real-time measurements. This can be done by using synchrophasor measurements from Phasor Measurements Units (PMUs). PMUs form part of the new Wide Area Monitoring, Protection and Control (WAMPAC) schemes proposed for power system grid visualization, monitoring and System Integrity Protection Schemes (SIPS). In comparison with Supervisory Control and Data Acquisition (SCADA) systems, PMUs are capable of providing time synchronized real-time measurements up to 200 frames per second (fps) for a system frequency of 50 Hz or 240 fps for a 60 Hz system frequency. On the contrary, SCADA-based measurements are unsynchronized and the measurements are polled only every 2-10 seconds.

Voltage stability is that property of a power system to maintain acceptable voltage profile at all the buses in the system under normal operating conditions and after being subjected to a disturbance. Voltage stability analysis methods based on synchrophasor measurements have been proposed in [2]-[7]. They serve as improvements over traditional methods based on P-V and V-Q curves [8],[9], load flow analysis-based indices [10]-[12], sensitivity analysis [13]-[15], and local measurements-based indices [16]-[20]. These traditional methods are cumbersome, and difficult to implement in real-time for practical systems. Also, most of the traditional methods are based on the calculation of the load flow Jacobian. The load flow calculation is usually assumed to diverge at the point of voltage collapse. However, the load flow may also diverge for stable conditions. Furthermore, the traditional methods do not take into account the system dynamics with respect to dynamic loads, transformer Under-Load Tap-Changers (ULTC), and generator Over Excitation Limiters (OXLs).

The synchrophasor-based voltage stability assessment methods in the existing literature [2]-[7] make use of Thevenin-equivalent estimation methods which are generally complex, difficult to implement in practical systems, and are based on the assumption that the system remains unchanged during two successive data acquisition period required for calculating the Thevenin equivalent voltage and impedance respectively. This is practically untenable since the system is usually changing especially during disturbances.

Also, the methods in the existing literature based on synchrophasors did not make use of actual measurements from PMUs. Rather, assumptions were made that synchrophasor measurements were available, and are equivalent to the time-domain measurements from power system simulation packages like DIgSILENT PowerFactory, PSCAD, SimPowerSystem, and PSS/E. However, what makes synchrophasor measurements unique from other measurement types is the estimation algorithm used, the filter type, message reporting rates, data transfer, and compliance to measurement/performance requirements based on the approved standards such as the IEEE C37.118 standard [21].

This paper intends to address some of the above-mentioned limitations by making use of actual synchrophasor measurements in the implementation of the less complex algorithms proposed in this study.

Authorized licensed use limited to: Cape Peninsula University of Technology. Downloaded on July 28,2020 at 15:02:11 UTC from IEEE Xplore. Restrictions apply.

Therefore, the contribution of this paper can be summarised as:

i. The extension of previous work by the authors [22] through the derivation of new generator-based indices for real-time Voltage Stability (VS) analysis.
ii. The formulation of wide area VS indices based on the concept of Voltage Control Areas (VCAs) and Reactive Power Reserve Basins (RPRBs).
iii. Comparison of existing VSA indices with the proposed indices.
iv. The use of actual synchrophasor measurements synchronized to the GPS and streamed onto a communication network infrastructure.
v. The design and implementation of a real-time synchrophasor-based testbed for testing and validating the proposed VSA indices.

The rest of this paper is organised as follows. Section 2 presents an overview of the proposed algorithms. The real-time implementation of the proposed algorithms is described in Section 3. Section 4 presents and discusses the results obtained. Section 5 summarises the contribution of this paper and provides some recommendations.

2 Overview of the Proposed Algorithms

2.1 Overview of the proposed derived indices

Voltage instability in power systems is primary caused by the inability of the combined generation and transmission systems to supply the required reactive power demand [9],[23]. This could be as a result of loss of voltage control or due to transformer Under-Load Tap-Changers (ULTCs) and shunt capacitors reaching their limits. In the analysis of a power system's ability to remain in equilibrium during steady-state condition or to regain acceptable level of equilibrium after a disturbance, the power system network can be partitioned into coherent load buses referred to as Voltage Control Areas (VCAs).

Similarly, the synchronous generators in the power system network can be clustered into Reactive Power Reserve Basins (RPRBs) based on the VCA to which they are providing reactive power support [23],[24]. The key generator within each respective RPRB can be identified and used as an indication of the system's status and margin to voltage instability [25]-[27]. The available reactive power reserve on the synchronous generators is obtained with respect to the system's voltage collapse point. This is known as the Effective Generator Reactive Power Reserve (EGRPR) [27]-[29]. This is in contrast to the Technical Generator Reactive Power Reserve (TGRPR) based on the generator capability curve as specified by the manufacturer. Although, the maximum power rating of generators can be obtained from the manufacturer's datasheet, the use of these maximum parameters can lead to misleading results [28],[29]. This is because at the voltage collapse point, not all the reactive power specified by the capability curve is available for voltage control. Also, the dynamic interaction of individual generators with other generators is not considered during the factory test used in defining the generator capability curve.

The rest of this section presents the voltage stability indices based on the principle of the EGRPR available in a large interconnected power system.

2.2 Effective generator reactive power reserve index

The EGRPR index is defined as the difference between the generator's maximum reactive power at the voltage collapse point and the reactive power at an operating point [27]-[29].

The maximum reactive power supplied by a generator is given by [9]:

$$Q_{g\max} = -\frac{V_g^2}{X_s} + \sqrt{\frac{V_g^2 I_{fd\max}^2}{X_s^2} - P_{g\max}^2} \qquad (1)$$

From (1), the EGRPR is:

$$EGRPR = Q_{g\max}^c - Q_{gk} \qquad (2)$$

where $Q_{\max}^c$ is the maximum generator reactive power at the voltage collapse point, Q_k is the generator reactive power at the current operating time *k*, $I_{fd\max}$ is the generator maximum field current at the voltage collapse point.

From (2), the Real-Time Voltage Stability Assessment (RVSA) index available at the *ith* generator is:

$$RVSA_{Q,i} = \left(\frac{Q_{g\max i}^c - Q_{gki}}{Q_{g\max i}^c} \right) \times 100\,\% \qquad (3)$$

$$RVSA_{Q,i} = \left(1 - \frac{Q_{gki}}{Q_{g\max i}^c} \right) \times 100\,\% \qquad (4)$$

where $Q_{g\max i}^c$ is the maximum reactive power on the *ith* generator at the voltage collapse point, Q_{gki} is the reactive power on the *ith* generator at the current operating time *k*.

2.3 Effective generator field current reserve index

An Effective Generator Field Current Reserve (EGFCR) index derived from the generator reactive power reserve is obtained using (1) [22].

At the voltage collapse point, EGFCR = 0, as $Q_{g\max i}^c = Q_{gk}$, $P_{g\max i}^c = P_{gk}$ at this point, then

$$-\frac{V_g^2}{X_s} + \sqrt{\frac{V_g^2 I_{fd\max}^2}{X_s^2} - P_{g\max}^2} = -\frac{V_g^2}{X_s} + \sqrt{\frac{V_g^2 I_{fdk}^2}{X_s^2} - P_{gk}^2} \qquad (5)$$

$$I_{fd\max}^c = I_{fdk} \qquad (6)$$

This forms the basis of the EGFCR index and it is defined as the difference between the maximum field current of the generator at the voltage collapse point and the generator field current at the *kth* operating time.

This is given mathematically as:

$$EGFCR = I_{fd\max}^c - I_{fdk} \qquad (7)$$

where $I_{fd\max}^c$ is the maximum generator field current at the voltage collapse point, I_{fdk} is the generator field current at the current operating time *k*.

Authorized licensed use limited to: Cape Peninsula University of Technology. Downloaded on July 28,2020 at 15:02:11 UTC from IEEE Xplore. Restrictions apply.

From (7), the Real-Time Voltage Stability Assessment (RVSA) index derived from the field current of the *ith* generator is given as [22]:

$$RVSA_{Ifd,i} = \left(\frac{I^{c}_{fd\,\max i} - I_{fdki}}{I^{c}_{fd\,\max i}} \right) \times 100\ \% \tag{8}$$

$$RVSA_{Ifd,i} = \left(1 - \frac{I_{fdki}}{I^{c}_{fd\,\max i}} \right) \times 100\ \% \tag{9}$$

where I_{fdki} is the *ith* generator field current at the current operating time *k*.

2.4 Effective Generator Stator Current Reserve index

An Effective Generator Stator Current Reserve (EGSCR) index derived from the generator reactive power reserve is proposed.

The maximum reactive power based on the generator stator current is given as [9]:

$$Q_{ga} = \sqrt{V_g^2 I_a^2 - P_{ga}^2} \tag{10}$$

where P_{ga} and Q_{ga} are the generator real and reactive powers, I_a is the generator stator current.

The maximum reactive power at the voltage collapse point is given as:

$$Q_{ga\max} = \sqrt{V_g^2 I_{a\max}^2 - P_{ga\max}^2} \tag{11}$$

where $P_{ga\max}$ and $Q_{ga\max}$ are the maximum generator real and reactive powers, $I_{a\max}$ is the maximum generator stator current.

At the voltage collapse point, EGSCR = 0, as $Q^{c}_{ga\max i} = Q_{gak}$, $P^{c}_{ga\max i} = P_{gak}$ at this point, then

$$\sqrt{V_g^2 I_{a\max}^2 - P_{ga\max}^2} = \sqrt{V_g^2 I_{ak}^2 - P_{gak}^2} \tag{12}$$

where I_{ak} and P_{gak} are the generator stator current and the real power respectively.

From (12),

$$I^{c}_{a\max} = I_{ak} \tag{13}$$

The above derivation forms the basis of the proposed EGSCR index and it is defined as the difference between the maximum stator current of the generator at the voltage collapse point and the generator stator current at the *kth* operating time.

This is given mathematically as:

$$EGSCR = I^{c}_{a\max} - I_{ak} \tag{14}$$

where $I^{c}_{a\max}$ is the maximum generator stator current at the voltage collapse point, I_{ak} is the generator stator current at the current operating time *k*.

From (14), the Real-Time Voltage Stability Assessment (RVSA) index derived from the stator current of the *ith* generator is proposed as:

$$RVSA_{Ia,i} = \left(\frac{I^{c}_{a\max i} - I_{aki}}{I^{c}_{a\max i}} \right) \times 100\ \% \tag{15}$$

$$RVSA_{Ia,i} = \left(1 - \frac{I_{aki}}{I^{c}_{a\max i}} \right) \times 100\ \% \tag{16}$$

where I_{aki} is the *ith* generator stator current reserve at the current operating time *k*.

For a large interconnected power system with multiple generators, the load buses in the power system can be partitioned into VCAs, and the generators providing reactive power support for these VCAs can be clustered to form RPRBs for each corresponding VCA. The key generator in these RPRBs can then be used to predict the state of the power system and its margin to voltage collapse.

On the basis of the above, the formulations for a large interconnected power system are proposed as given in the derivations below.

$$RVSA_{Q,sys} = \min_{i \in sys} \left\{ RVSA_{Q,i} \right\} = \min_{i \in sys} \left\{ \left(1 - \frac{Q_{gki}}{Q^{c}_{g\max i}} \right) \times 100\ \% \right\} \tag{17}$$

$$RVSA_{Ifd,sys} = \min_{i \in sys} \left\{ RVSA_{Ifd,i} \right\} = \min_{i \in sys} \left\{ \left(1 - \frac{I_{fdki}}{I^{c}_{fd\max i}} \right) \times 100\ \% \right\} \tag{18}$$

$$RVSA_{Ia,sys} = \min_{i \in sys} \left\{ RVSA_{Ia,i} \right\} = \min_{i \in sys} \left\{ \left(1 - \frac{I_{aki}}{I^{c}_{a\max i}} \right) \times 100\ \% \right\} \tag{19}$$

These RVSA indices are used in the computation of the system's margin to voltage collapse. The RPRB with the minimum index indicates the state of the system and its proximity to voltage collapse. The simplification of these indices allows for their application in practical networks in real-time using synchrophasor measurements from PMUs.

3 Real-Time Implementation

The testing and validation of the proposed generator-derived VS indices were carried out using industrial-grade equipment comprising of the Real-Time Digital Simulator (RTDS®), Phasor Measurement Units (PMUs), RTDS-GTNET-PMU, Phasor Data Concentrator (PDC) SEL-5073, Synchrophasor Vector Processor (SVP) SEL 3378, GPS satellite clock, and communication network infrastructure as shown in Fig. 1.

The RTDS® was used in combination with the RSCAD software for modeling and simulating the power system network. The measurements from the generators and load buses of interest were streamed as IEEE C37.118 synchrophasor measurements onto an Ethernet network.

The synchrophasor measurements were obtained from the GTNET-PMU, and from external PMUs connected to the RTDS via signal amplifiers. The SVP served as a substation PDC and also as a Programmable Logic Controller (PLC) for executing the proposed algorithms using the IEC 61131-3 programming language.

The SEL-5073 was used as a SuperPDC at the central control centre. It collected and time-aligned the measurements from geographically-dispersed stations according to their time-stamps. These time-aligned measurements can be made available to other applications, and also archived for offline analysis.

Authorized licensed use limited to: Cape Peninsula University of Technology. Downloaded on July 28,2020 at 15:02:11 UTC from IEEE Xplore. Restrictions apply.

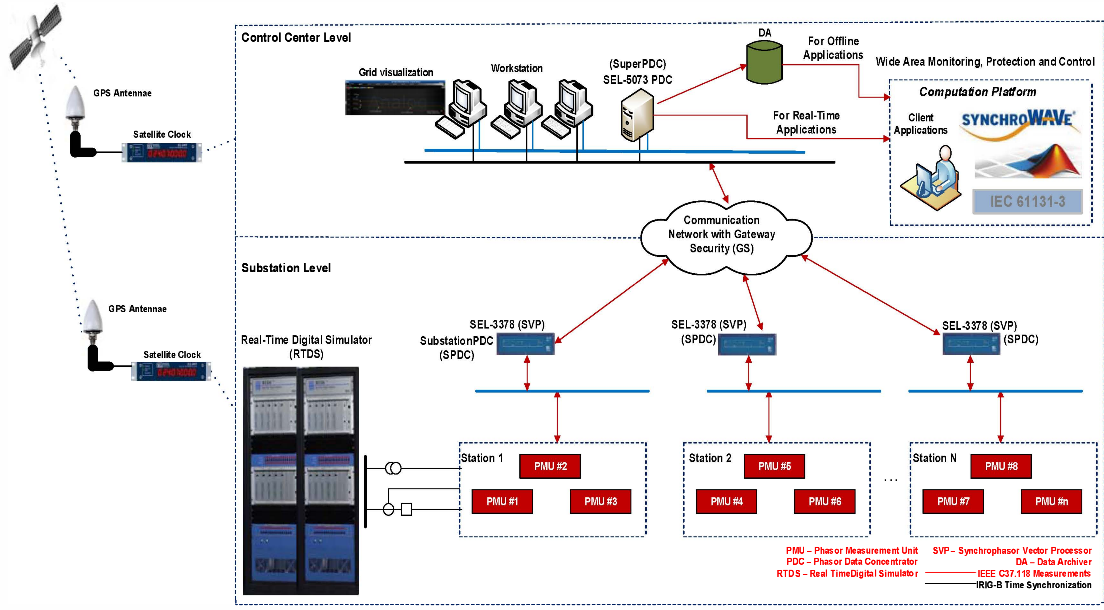

Fig. 1. Implementation architecture of the real-time lab-scale testbed used.

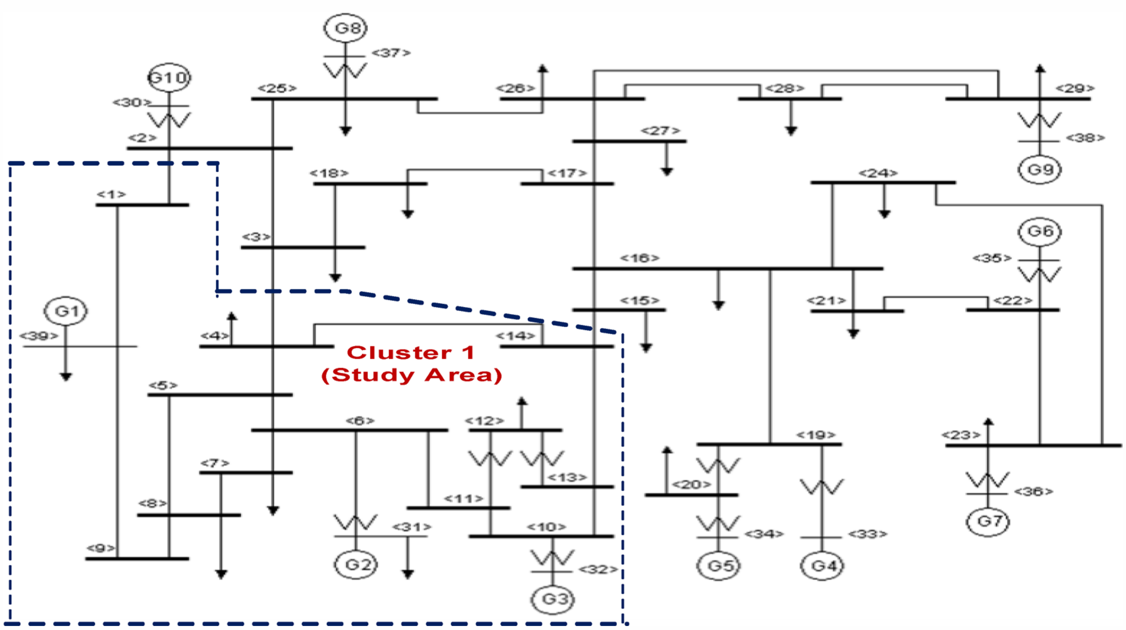

Fig. 2. New England 39-bus benchmark test system [30].

3.1 Modelling

The New England 39-bus benchmark test system [30] was modelled using RSCAD software. This test system is made up of 39 buses, 34 transmission lines, 12 transformers, and 19 loads with a total load demand of 6150 MW, while the total generated power from 10 synchronous machines is 6192 MW. The synchronous generators were equipped with IEEE Type-1 excitation systems and governors. Fig. 2 shows the single line diagram of the test system.

3.2 Simulations

Various operating conditions were simulated using the lab-scale testbed implemented. The case studies considered included:

- Case study 1: Small disturbance voltage stability simulation involving small perturbation in load demand.
- Case study 2: Large disturbance voltage stability involving *N*-1, *N*-2 transmission line and generator contingencies respectively.
- Case study 3: A combination of load increase, the long-term dynamics of transformer ULTC action and the operation of generator Over Excitation Limiters (OXLs) respectively.

Authorized licensed use limited to: Cape Peninsula University of Technology. Downloaded on July 28,2020 at 15:02:11 UTC from IEEE Xplore. Restrictions apply.

The results obtained for the afore-mentioned case studies are presented in Section 4.

4 Results and Discussion

In this section, results obtained for the case studies used in the evaluation of the proposed real-time voltage stability assessment algorithms are presented.

4.1 Case study 1

The first case study involved increased system loading at load buses 4, 7, 8, and 12. A 7.5% load increase from the base case was carried out every 60 s. Buses 4, 7, 8, and 12 were used because P-V curve analysis carried out using DIgSILENT PowerFactory showed that these load buses have a similar voltage collapse problem and can be assigned to a common Voltage Control Area (VCA). This is as shown in Fig. 3.

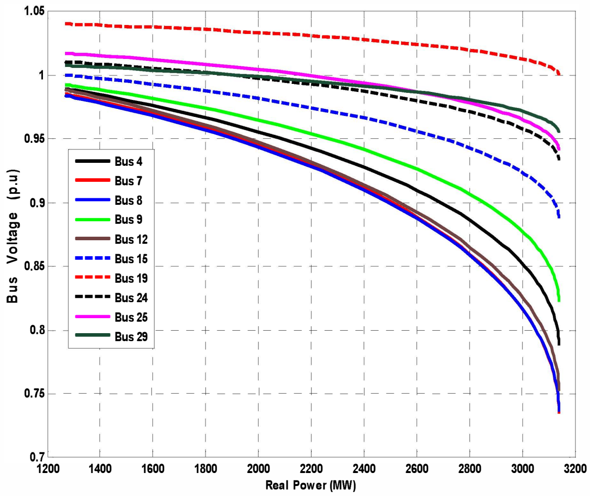

Fig. 3. P-V curve analysis for the test system.

As shown in Fig. 3, buses 4, 7, 8, and 12 belong to the same VCA since they experienced voltage collapse for the same system disturbance. Similarly, Fig. 4 shows the plots of the generator field and stator currents respectively.

Tl
cc

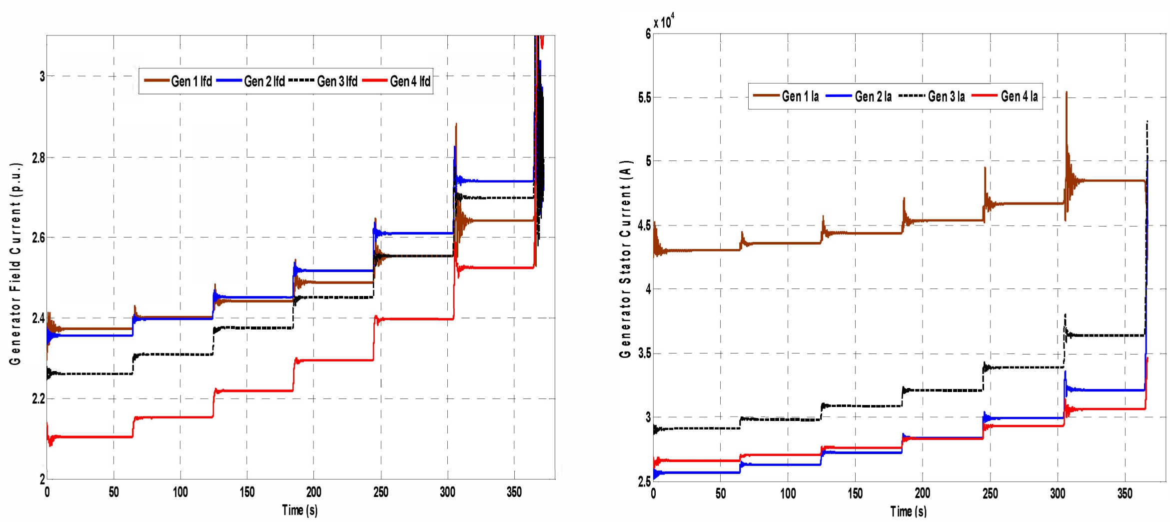

(a) (b)

Fig. 4. Case study 1: (a) plots of generator field currents; and (b) plots of generator stator currents detailing increased system loading.

Reserve Basin (RPRB). The generators within this group were obtained through real-time simulation to include generators G1, G2, and G3. Generator G4 was added to the result even though it belonged to a neighbouring RPRB. However, it was observed that G4 did not exhaust its reactive power reserve for the considered study VCA.

Fig. 5 shows the real-time plot obtained for the indices based on the generator reactive power reserve (EGRPR), generator field current reserve (EGFCR), and the generator stator current reserve (EGSCR). It can be seen from these results that the $RVSA_{Ia}$ index obtained from the EGSCR gave the most consistent indication of the state of the system as the system condition changes. Next to this in terms of performance was the $RVSA_{Ifd}$ index from the EGFCR. The $RVSA_{Q}$ index based on the EGRPR showed a steep change as the system condition changed.

4.2 Case study 2

The second case study involved transmission line and generator contingencies respectively. The test system was able to withstand N-1 transmission line and generator (G2-G10) contingencies respectively. A cascading scenario involving the loss of transmission line (Line 15-16) and generator (G6) outage, combined with increased system loading was demonstrated. Fig. 6 shows the result obtained for this simulation in real-time. It was observed that the various indices were able to indicate the various system conditions and the voltage collapse point.

Table I shows the RVSA margins and the existing indices (LQP and FVSI) proposed by [17]-[18] obtained for various contingencies. It can be seen from these results that the $RVSA_{Ia}$ index obtained from the generator stator current (EGSCR) gave the most consistent indication of the state of the system as the system condition changed.

Authorized licensed use limited to: Cape Peninsula University of Technology. Downloaded on July 28,2020 at 15:02:11 UTC from IEEE Xplore. Restrictions apply.

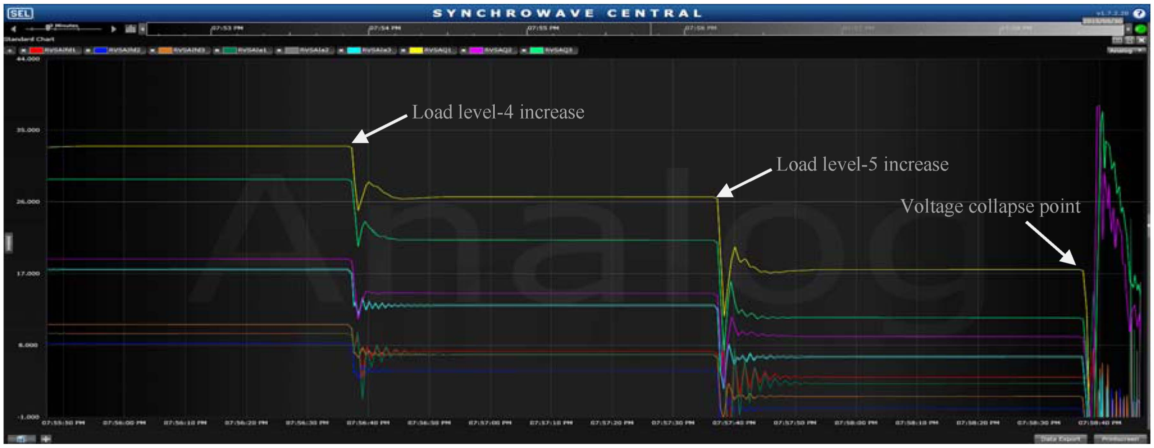

Fig. 5. Case study 1: Real-time plots indicating small disturbance voltage instability using increased system loading.

Table I. Case study 2: Voltage stability indices for various transmission line and generator contingencies.

Contingency	$FVSI_{3-4}$ (Line 3-4)	LQP_{3-4} (Line 3-4)	$RVSA_{Q,2}$ (%)	$RVSA_{Q,3}$ (%)	$RVSA_{Ifd,2}$ (%)	$RVSA_{Ifd,3}$ (%)	$RVSA_{Ia,2}$ (%)	$RVSA_{Ia,2}$ (%)
Loss of Line 3-4	0.137	0.178	26.57	41.49	13.11	16.13	24,25	23.77
Loss of Line 14-15	0.154	0.195	27.27	40.51	12.82	15.65	24.08	23.43
Loss of Line 15-16	0.232	0.267	31.63	45.40	11.52	14.08	20.82	19.98
Loss of Generator G6	0.173	0.247	25.58	32.81	8.06	10.16	16.23	15.86
Loss of Generator G7	0.170	0.252	23.36	36.44	7.69	10.55	17.06	16.51
Loss of Generator G8	0.173	0.247	25.58	32.81	8.06	10.16	16.23	15.86
Loss of Generator G9	0.183	0.275	12.99	28.49	6.72	9.47	14.19	13.48

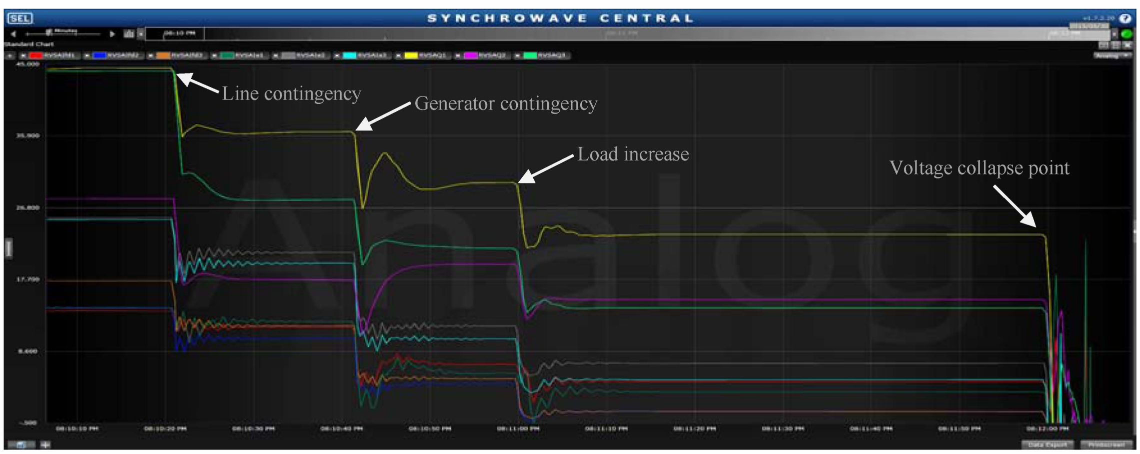

Fig. 6. Case study 2: Real-time plots of generator-derived indices for increased loading conditions, line and generator contingencies.

4.3 Case study 3

This case study involved transmission line and generator contingencies coupled with the dynamics of transformer Under-Load Tap-Changer (ULTC) and generator OXL respectively. The transformer between buses 11 and 12 was modified to include an ULTC. Similarly, OXLs were added to generators G2 and G3. The parameters for the ULTC and OXL were calculated based on the recommendations from [30], and are presented in the Appendices.

The loads at buses-4, 7, 8, 12 were increased by 7.5% every 60 s. Fig. 7 illustrates the simulation carried out in real-time. As a result of the voltage decline due to the transmission line contingency, the transformer ULTC at bus 12 starts to tap in an attempt to restore the bus voltage to its reference point. This results in an increase in the field current and reactive power supplied by the generators in the RPRB relating to this VCA.

The voltage at bus 12 continues to decline as a result of further tapping of the transformer ULTC and the load increase in its VCA. At time t = 180 s, the key generator at this RPRB (G3) reaches its field current limit and causes the OXL at G3 to operate. This ramps down the output of G3 to the acceptable limit.

The consequence of this is that G3 changes from a PV source and becomes a PQ bus. At the point of OXL action, the indices from the generator reactive power (EGRPR) and the generator field current (EGFCR) fail as can be seen from the plots in Fig. 7. Despite the impending voltage collapse, the indices based on the EGRPR and the EGFCR began to show recovery, acting like the system was recovering from the instability. However, the index based on the EGSCR continued to function unaffected by the OXL action.

Authorized licensed use limited to: Cape Peninsula University of Technology. Downloaded on July 28,2020 at 15:02:11 UTC from IEEE Xplore. Restrictions apply.

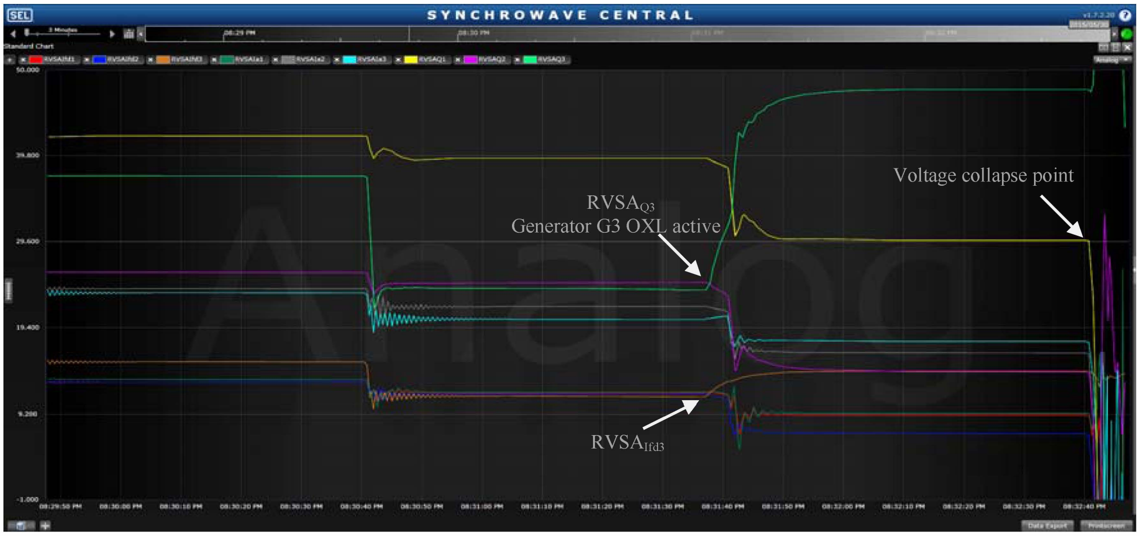

Fig. 7. Case study 3: Real-time plots of generator-derived indices for increased loading conditions, ULTC and OXL dynamics.

5 Conclusion

This paper presented three generator-derived indices for voltage stability assessment in power systems. The indices were based on the reactive power reserve, field current reserve, and stator current reserve of the key generators within each RPRB in a large interconnected power system. Comparison carried out on the various generator-derived indices showed that the index based on stator current reserve (EGSCR) from the key generator provided the best indication of the power system state and margin to voltage collapse. The limitation of the generators through the action of their OXLs resulted to the failure of the EGRPR and EGFCR indices. Another shortcoming of the EGRPR index was that its response was steep and could give a false sense of security. However, the index based on EGSCR showed consistency for all the cases it was applied to. The index based on EGSCR is promising, uses fewer PMU measurements, less measurement sensors are required, reduced project/maintenance costs, and it is suitable for real-time application for providing online situational awareness of the power system.

Future work intends to apply these indices as inputs to the system monitoring element of System Integrity Protection Schemes (SIPS) designed for preserving the integrity of the grid during voltage instability in order to prevent system collapse and cascading blackouts.

Appendix A

The OXL parameters at generators G2 and G3 are calculated based on the recommendations from [9]. The calculated parameters are presented in Tables AI and AII respectively.

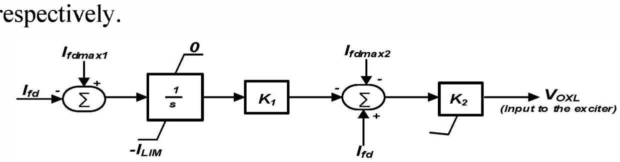

Fig. A1. Block diagram of the OXL at generator G3.

Table AI. Generator G2 OXL parameters.

I_{fdmax1} (p.u.)	I_{fdmax2} (p.u.)	I_{LIM} (p.u.)	K_1	K_2
2.47695	3.7744	11.0	0.248	12.6

Table AII. Generator G3 OXL parameters.

I_{fdmax1} (p.u.)	I_{fdmax2} (p.u.)	I_{LIM} (p.u.)	K_1	K_2
2.352	3.584	11.0	0.248	12.6

where I_{fd} is the generator field current at the current operating time, $I_{fd\max 1}$ and $I_{fd\max 2}$ are the maximum field current limits for stages 1 and 2 of the generator OXL respectively. Further details are available in [9].

Appendix B

The ULTC parameters used for the transformer between buses 11 and 12 are given in Table BI.

Table BI. Transformer ULTC parameters.

Dead band (Vp.u.)	Tap range (steps)	Step size (p.u.)	Time delay for 1st tap (s)	Time delay for subsequent taps (s)
± 1%	±16	0.00625	30 .0	5 .0

References

[1] Final report on the August 14, 2003 blackout in the United States and Canada: causes and recommendations. (2004). U.S.–Canada Power System Outage Task Force.

[2] L. Warland, A.T. Holen. (2002). Estimation of distance to voltage collapse: testing and algorithm based on local measurements. *Proc. 14th Power System Computation Conference Sevilla (Spain)*, Paper s38p03.

[3] M. Larsson, C. Rehtanz, J. Bertsch. (2003). Real-time voltage stability assessment of transmission corridors. *Proceedings of IFAC Symposium on Power Plants and Power Systems Seoul, S. Korea*. pp. 1-6.

[4] S. Corsi, G.N. Taranto. (2008). A real-time voltage instability identification algorithm based on local phasor measurements. *IEEE Transactions on Power Systems. 23(3)*, pp. 1271–1279.

[5] G. Mevludin, T. Van Cutsem. (2009) Wide-area detection of voltage instability from synchronized phasor measurements. Part I: Principle. *IEEE Transactions on Power Systems. 24(3)*, pp. 1408-1416.

Authorized licensed use limited to: Cape Peninsula University of Technology. Downloaded on July 28,2020 at 15:02:11 UTC from IEEE Xplore. Restrictions apply.

[6] R. Sodhi, S.C. Srivastava, S.N. Singh. (2012). A simple scheme for wide area detection of impending voltage instability. *IEEE Transactions on Smart Grid. 3(2)*, pp. 818-827.
[7] J.H. Liu, C.C. Chu. (2014). Wide-area measurement-based voltage stability indicators by modified coupled single-port models. *IEEE Transactions on Power Systems. 29(2)*, pp.756-764.
[8] V. Ajjarapu, B. Lee . (1992). Bifurcation theory and its application to nonlinear dynamical phenomena in an electrical power system. *IEEE Transactions on Power Systems. 7*, pp. 424-431.
[9] P. Kundur. (1994). *Power system stability and control*. McGraw-Hill.
[10] P. Kessel, H. Glavitsch, (1986). Estimating the voltage stability of a power system. *IEEE Transactions on Power Delivery. 1(3),* pp. 346-354.
[11] H.G. Kwatny, A.K. Pasrija, L.Y. Bahar. (1986). Static bifurcations in electric power networks: Loss of steady-state stability and voltage collapse. *IEEE Transactions on Circuits and Systems. 33(10),* pp. 981-991.
[12] S.G. Ghiocel, J.H. Chow. (2014). A power flow method using a new bus type for computing steady-state voltage margins. *IEEE Transactions on Power Systems,* 29(2), pp. 958-965.
[13] O.O. Obadina, G.J. Berg. (1988). Determination of voltage stability limit in multimachine power systems. *IEEE Transactions on Power Systems, 3* (4), pp. 1545-1553.
[14] S. Greene, I. Dobson, F.L. Alvarado. (1999). Contingency ranking for voltage collapse via sensitivities from a single nose curve, *IEEE Transactions on Power Systems, 14(1)*, pp. 232-240.
[15] A. Berizzi, Y.G. Zeng, P. Marannino, A. Vaccarini, P.A. Scarpellini. (2002). A second order method for contingency severity assessment with respect to voltage collapse. *IEEE Transactions on Power Systems, 15 (1)*, pp. 81-87.
[16] M. Moghavvemi, O. Faruque. (1998). Real-time contingency evaluation and ranking technique. *IEE Proc. Gener. Transm. Distrib.,*, *145(5)*, pp. 517-524.
[17] S.Y.A. Mohamed , G.B. Jasmon . (1989). A static voltage collapse indicator using line stability factors. *Journal of Industrial Technology*, *7*, pp. 73–85.
[18] I. Musirin, T.K.A. Rahman . (2002). Online voltage stability based contingency ranking using fast voltage stability index (FVSI). *In Proceedings of IEEE/PES Transmission and Distribution Conference and Exhibition. 2*, pp. 118-1123.
[19] V. Balamourougan, T.S. Sidhu, M.S. Sachdev. (2004). Technique for online prediction of voltage collapse. *IEEE Proceedings in Generation, Transmission and Distribution. 151(4)*, pp. 453-460.
[20] J.E. Tobon, R.E.C. Gutierrez, J.M. Ramirez. (2014). Voltage collapse detection based on local measurements. *Electric Power Systems Research. 107*, pp. 77-84.
[21] IEEE Standard for synchrophasor measurement for power systems, IEEE Standard C37.118.1-2011, 2011.
[22] A.C. Adewole, R. Tzoneva. (2014) Real-time deployment of a novel synchrophasor-based voltage stability assessment algorithm. *International Review of Electrical Engineering. 9(5),* pp. 1021-1033.
[23] R.A. Schlueter. (1998). A voltage stability security assessment method. *IEEE Transactions on Power Systems. 13,* pp. 1423-1438.
[24] B. Avramovik, L.H. Fink. (1992). Real-time reactive security monitoring. *Transactions on Power Systems.* 7(1), pp. 432-437.
[25] C.W. Taylor, R. Ramanathan. (1998) BPA reactive power monitoring and control following August 10, 1998 power failure. *In proc. VI Symp. Specialists Elect. Oper. Expansion Planning, Salvador, Brazil.*
[26] L. Bao, Z. Huang, W. Xu. (2003). Online voltage stability monitoring using VAR reserves. *IEEE Transactions on Power Systems. 18*, pp. 1461-1469.
[27] Y.H. Choi, S. Seo, S. Kang, B. Lee. (2011). Justification of effective reactive power reserves with respect to a particular bus using linear sensitivity. *IEEE Transactions on Power Systems. 26(4)*, pp. 2118-2124.
[28] B. Leonardi, V. Ajjarapu. (2008). Investigation of various generator reactive power reserve (GRPR) definitions for online voltage stability/Security assessment. *Proceedings of 2008 IEEE PES General Meeting,* Tampa, USA. *554*, pp. 1-7.
[29] O.A. Mousavi, M. Bozorg, R. Chekaoui. (2013) Preventive reactive power management for improving voltage stability. *Electric Power System Research. 96*, pp. 36-46.
[30] M.A. Pai. (1989). *Energy function analysis for power system Stability*. Boston: Kluwer Academic Publishers, pp. 223-227.

AUTHORS BIOS AND PHOTOGRAPHS

Adeyemi Charles Adewole obtained his B.Eng. (Hons.) in Electrical and Electronics Engineering from the Federal University of Technology, Akure in 2006, and his Master's Degree in Electrical Engineering from the Cape Peninsula University of Technology (CPUT) in 2012.

He is currently a doctoral student and research assistant at the Centre for Substation Automation and Energy Management Systems (CSAEMS) at CPUT. His research interests are in power systems protection and automation, real-time digital simulations, power system stability, wide area monitoring, protection, and control.
Mr. Adewole is a Member of the Institution of Engineering and Technology (IET) UK, and a Member of the Institute of Electrical and Electronics Engineers (IEEE) USA.

R Tzoneva has M.Sc and Ph.D in Electrical Engineering (control specialization) from the Technical University of Sofia (TUS) and was an Associate Professor at the Bulgaria Academy of Sciences, Institute of Information Technologies between 1982 and 1992. Since 1998, she has been working as a Professor at the Department of Electrical Engineering, Cape Peninsula University of Technology, Cape Town. She is the Leader of the niche-area Real Time Distributed Systems (RTDS) and the Centre for Substation Automation and Energy Management Systems supported by the South African National Research Foundation (NRF). Her research interest is in the field of optimal and robust control design, optimization of linear and nonlinear systems, energy management systems, real-time digital simulations, and parallel computation.
Prof. Tzoneva is a Member of the Institution of Electrical and Electronics Engineers (IEEE) USA.

Presenting author: The paper will be presented by A.C. Adewole.

Authorized licensed use limited to: Cape Peninsula University of Technology. Downloaded on July 28,2020 at 15:02:11 UTC from IEEE Xplore. Restrictions apply.